



Kinematic interpretation of shearband boudins: New parameters and ratios useful in HT simple shear zones

Jorge Pamplona^{a,*}, Benedito C. Rodrigues^b

^aCentro de Investigação Geológica, Ordenamento e Valorização de Recursos, Universidade do Minho, Campus de Gualtar, 4710-057 Braga, Portugal

^bCentro de Geologia da Universidade do Porto, Rua do Campo Alegre, 687, 4169-007 Porto, Portugal

ARTICLE INFO

Article history:

Received 30 December 2009

Received in revised form

12 October 2010

Accepted 27 October 2010

Available online 12 November 2010

Keywords:

Shearband boudin

Geometric parameters

HT simple shear zone

Kinematics

ABSTRACT

Shearband boudins (asymmetric boudins showing slip along the inter-boudin surface, which is synthetic with respect to the bulk shear sense) are ubiquitous and well exposed in HT simple shear zones. The present work aims to extend the methodology of analysis of shearband boudins developed by Goscombe and Passchier (2003). Such shearband boudins represent complex objects that require an adequate methodology for unambiguous kinematic interpretation.

We propose new geometric parameters (Bbs , $B-t$, c' , D' , d , ψ') in order to describe and identify, with confidence, the kinematics of boudinage in this particular geological framework. The key-observation for kinematic interpretation in simple shear regimes is the boudin axis (Lb) that is commonly present, excluding the necessity to identify the regional stretching lineation (Lx) in the metasedimentary matrix. In monoclinic HT simple shear zones, this approach involves the use of a local displacement plane (Sx), which is always normal to the boudin axis (Lb).

© 2010 Elsevier Ltd. All rights reserved.

1. Introduction

The terms boudin and boudinage were used for the first time by Lohest et al. (1908) to describe sausage-like structures occurring in psammite layers of the Lower-Devonian metasedimentary series in the Mardassonn quarry, near Bastogne (Ardenne, Belgium). In fact, these original structures look like boudins, but resulted from a sequence of deformation episodes that generated “textbook examples of mullions” (cf. Sintubin and Urai, 2007).

The concept of boudinage has evolved from a purely descriptive term, without any kinematic implications (e.g., Lohest et al., 1908; Wegman, 1932), passing through a kinematic approach (Cloos, 1947), to the actual kinematic definition highlighted by Price and Cosgrove (1990) and later adopted by Goscombe et al. (2004).

The placement of boudins in the universe of strained bodies in a ductile matrix may be taken as the response to the following question: what enables a body to be deformed as a boudin? This requires the consideration of several concepts, such as viscosity contrast, strain and mechanical constraints, external morphological axial ratios and deformation regimes (simple shearing vs. pure shearing).

* Corresponding author. Tel.: +351 253604307; fax: +351 253678206.
E-mail address: jopamp@dct.uminho.pt (J. Pamplona).

The difference in viscosity between the veins and the matrix has been cited as the major factor that determines the evolution of boudinage (Ghosh and Sengupta, 1999; Mandal et al., 2000; Bons et al., 2004; Goscombe et al., 2004; Treagus and Lan, 2004). Nevertheless, this statement is not sufficient to explain the generation of all types of boudins, and has been questioned in several studies. When structures, like foliation boudins are generated, authors like Mandal et al. (2000) admit the existence of boudin genesis at low viscosity contrast, while Arslan et al. (2008) suggest that genesis of foliation boudins may be independent of viscosity contrast. Indeed, such structures only have a certain geometric identity with boudins, and were generated in a distinct way.

In situations of high viscosity contrast, boudinage is controlled by the occurrence of fracturing with simultaneous shearing and extensional components, which affect the strained bodies in the ductile matrix (Mandal et al., 2000). These authors define different types of boudins, for high strength ratio between individual brittle and ductile layers, using the relationship between the tensile stress and the compressive stress, respectively, acting in brittle layers.

Analysis of boudinage usually considers bodies of infinite dimension. In Nature, this geometric condition cannot occur, and is rarely approximated. There is a shape ratio representing the limit at which the tabular structure ceases to generate boudins, and it will behave instead as a solid particle in ductile matrix, described by the models of Jeffery (1922) and Eshelby (1957). Theoretically, the

rotation of these bodies is locked only for very low a/c shape ratios (external morphological axis: a – short axes and c – long axes), giving rise to the possibility that boudinage will occur. Ghosh and Ramberg (1976) and Rambosek et al. (2005), discussing the influence of the a/c ratio on the rotation of elongate rigid inclusions, during combined pure and simple shear, confirmed the stabilization of long axes parallel to the shear plane when the a/c ratio reaches a suitable value.

As stated above, different authors, at different times, have different approaches to explain the boudinage phenomena. From this summary remains that the three major factors that control the boudinage are: the deformation regime (pure shearing vs. simple shearing), the external morphological axial ratio (shape ratio) and the viscosity contrast.

A methodology for boudin analysis was recently established by Goscombe et al. (Goscombe and Passchier, 2003; Goscombe et al., 2004). Nevertheless, this methodology does not clarify all the types of boudins, and, usually has application only in ideal geometric cases. Therefore, the present work results from the need to better define the criteria for interpreting the kinematics of boudins, extending the analysis to the case of HT simple shear zones and some ill-defined shearband boudins.

For the easiest perception of the use of boudins as kinematic indicators in simple shear zones, it is necessary to define geometric parameters that must be simple to record and combine. Frequently, the geometry of the boudins leads to an ambiguous interpretation of their kinematics. The proposed methodology seeks to overcome this limitation.

The approach developed uses field data from the sector of Salgosa that presents an excellent set of outcrops of different boudins. This sector is part of the Malpica-Lamego ductile shear zone (MLDSZ), a major crustal Variscan structure in the NW of the Iberian Peninsula (Rodrigues et al., 1999; Llana-Funez and Marcos, 2001; see Section 3.1).

2. Geometric analysis of boudins and significance of parameters

A recent boudin definition considers it as a body resulting from a process of disruption of layers, bodies or foliation planes within the rock mass as a response to extension along the enveloping surface (Goscombe et al., 2004).

There are other bodies with geometric affinities with boudins, but subjected to a different genetic interpretation. These are the cases of pseudo-boudins or misleading boudin-like structures referred to by Bons et al. (2004), for example mullions and sigmoidal structures.

Boudins can be classified into a kinematic and geometric scheme as proposed by Goscombe et al. (2004). Table 1 presents a summary of such classification.

2.1. Definition of parameters

In its simplistic form, the shearband boudin “anatomy” can be described as a parallelepiped body with four opposite sides two by two, whose edges are alternately acute and obtuse, referred herein, respectively, as the sharp tip (S-t) and blunt tip (B-t).

The geometric analysis as proposed by Goscombe and Passchier (2003) identifies the group of parameters that are described in Table 2 and Fig. 1. The most important parameters are L_b , L , W , θ , D and some relationships established between them (L/W , D/W , L/W vs. θ and D/W vs. θ).

In addition to the parameters highlighted as the most significant to shearband boudin analysis in Table 2, Goscombe et al. (2004) present a set of other parameters and related concepts used in boudin characterization. For the dependence with the inter-boudin surface (Sib), the concepts of slip sense (lateral displacement along Sib, with respect to bulk shear sense), vergence (relation between bulk shear sense and Sib inclination) and “drag” on Sib (sense of

Table 1
Classification of boudin types (adapted from Goscombe et al., 2004).



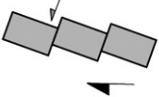
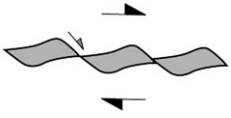
Kinematic class	Boudin block geometry	Boudin types	Geometric description of boudin
No slip along the inter-boudin surface	Symmetric	Torn 	Orthorhombic symmetry that is distinguished by the shape of interboudin surface: straight in torn boudins (with or without vein infill) and smooth for drawn boudins
		Drawn 	
		Domino (Etchecopar, 1977) 	
Slip along the inter-boudin surface	Asymmetric	Shearband (Swanson, 1992) 	Monoclinic symmetry with rounded and even sigma shape, and curvilinear inter-boudin surface
Synthetic slip			

Table 2
Most relevant geometric and kinematics parameters of boudins defined by Goscombe and Passchier (2003) and introduced in this work. Sb is the original surface of boudin block with host rock and represents the final external surface of boudin; Sib is the inter-boudin surface that means, either a discrete slip surface separating boudins or an imaginary surface between two adjacent boudins.

References	Parameters	Description
Parameters introduced by Goscombe and Passchier (2003)	Lb	Long axis of boudin, corresponding to the boudin edge, which materialises the rotation axis in simple shear
	L	Length of boudin measured parallel to Sb
	W	Width or thickness of boudin measured normal to Sb that is always equal or smaller than the original thickness of boudinage layer
	D	Lateral displacement between individual and adjacent boudins measured parallel to Sib
	θ	Acute angle between Sb and Sib quantifying boudin block shape
Parameters introduced in present work	c' type-I	Orientation of secondary synthetic shear plane ($\dot{\epsilon}$ structure) in which occurs the lateral displacement between adjacent boudins; includes D' and Sib
	D'	Inter-boudin displacement measured between adjacent boudins, along Sib; it is always lesser than D
	Bbs	Orientation of the boudin symmetry plane; contains the boudin axis (Lb) and is defined by the intersection points between the opposite sharp tips and the secondary synthetic shear plane (c')
	B-t	Blunt tip is the zone of boudin surface that corresponds to the development of a convexity at the interface boudin/matrix with c' type-I
	d	Measure of boudin internal asymmetry; line segment defined on the Bbs, between diametric opposite B-t, which are defined by its orthogonal projection on Bbs
	ψ'	Angular relationship that is measured in function of the opposite B-t positions

apparent drag on boudin face) are used. On this surface are also described the slickenlines, or mineral elongation lineations, (Lib), that are the expression of the movement within it. Angular relationships between geometrical entities, such as the degree of

departure from monoclinic symmetry (δ – the acute angle between the regional stretching lineation and the Lb), or the relative block rotation (α – the angle between envelope surface and Lb) or obliquity of the boudin train (ψ – the angle between Se and the

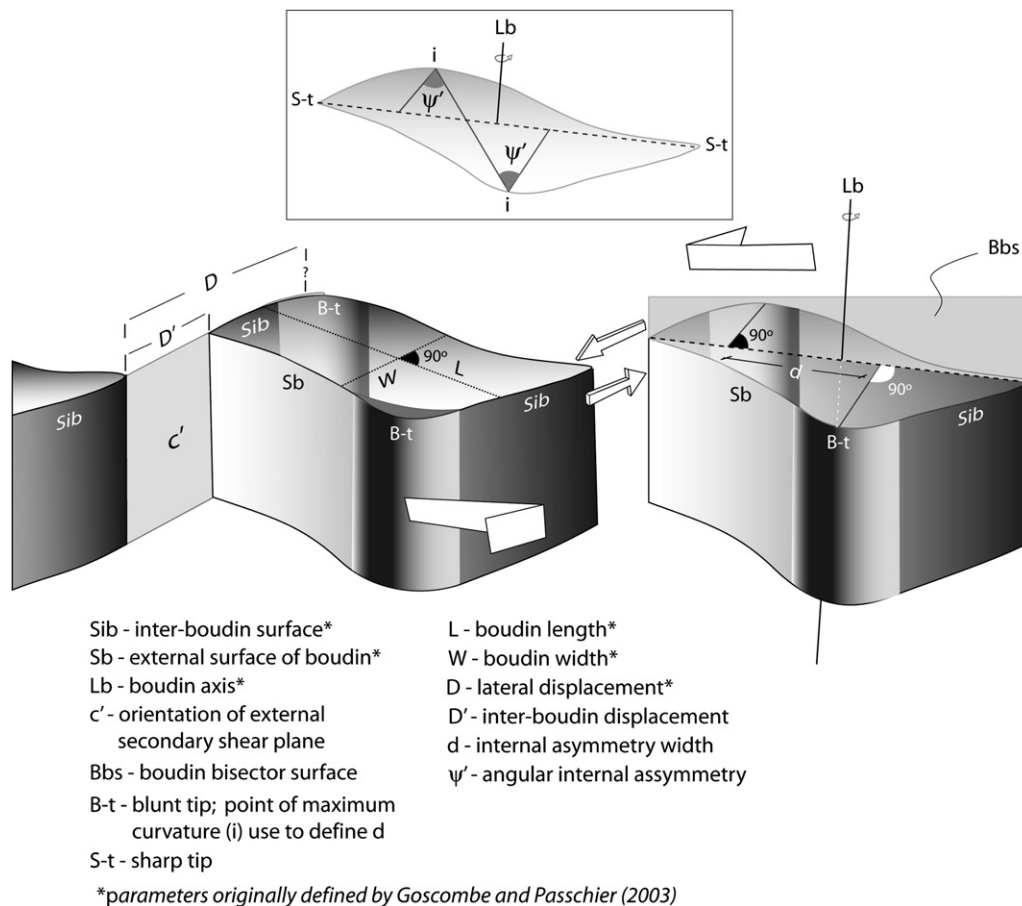


Fig. 1. Most important geometric parameters of shearband boudins in HT simple shear zones as defined by Goscombe and Passchier (2003) and in the present work. Bulk shear sense is sinistral. The geometry of these boudins departs from the one of an ideal symmetric body, whereby the identification of some parameters is of some practical difficulty, such as the measurement of D .

fabric attractor), are useful to describe a complete orientation of a boudin block. Goscombe et al. (2004) also propose other dimensional parameters, like the two components of extension (N – displacement normal and across S_{ib} and M – extension of boudinage parallel to S_e and normal to L_b).

The boudin analysis proposed in this work includes the measurement of the L_b orientation (Fig. 1), a parameter defined, but not explored, by Goscombe et al. (2004), as a fundamental element of the kinematic analysis in simple shear. In the area under study, L_b proved always to be perpendicular to a local displacement plane (S_x), which raises the question whether this relationship is exclusive to symmetries higher than triclinic (Goscombe et al., 2004; Reddy and Buchan, 2005) or is independent of the symmetry. S_x is defined in Fig. 2 as the plane that contains different lineations (stretching lineation in the host rock, mineral lineation along the inter-boudin plane, called L_{ib} by Goscombe et al. (2004), and mineral lineation on the boudin exterior surface, reworked as slickensides). S_x is the plane where the maximum asymmetry can be observed, therefore its normal (L_b) is inferred to be parallel to the vorticity axis.

The identification and measurement of the orientation of L_b , that corresponds to the vorticity axis (a relation valid to flows in simple shear), allows us to recognize that S_x statistically includes the direction of displacement in the shear plane, since S_x is always normal to L_b in simple shear (Fig. 2). This relationship is imposed by geometry and symmetry reasons (Neumann and Curie principles, Paterson and Weiss, 1961) and was broadly verified in fieldwork.

The L and W dimensional parameters are measured in two normal directions (Fig. 1). Nevertheless, their absolute orientations are not well constrained because the shearband boudins rarely correspond to a plane of unbiased measurement. In fact, the shearband boudins rarely show parallelepiped shapes, but,

commonly, they are irregular, curved and limited by incompletely exposed surfaces. As a consequence of this practical difficulty, a new orientation parameter B_{bs} (bisector boudin surface) was introduced, defined as the plane containing L_b and the line joining the two sharp tips of the shearband boudin.

A secondary synthetic shear plane associated with boudinage development can be identified that is distinct from the C' penetrative shearband cleavage related with pseudo-boudinage structure (Bosworth, 1984). This new parameter is denoted as c' type-I (Fig. 1), in order to avoid any confusion. The parameter c' type-I represents a kinematic surface, easy to recognize and measure, that includes S_{ib} (the inter-boudin surface), D (the distance between homologous points in two adjacent boudins) and D' (the separation between two adjacent boudins) – Fig. 1. The notation c' type-I is used to refer to the structure as well as to its orientation.

The surface morphology of boudins in HT shear zones departs significantly geometrically from the original tabular body surface. The most remarkable features are the sharp tips and the presence of two convex surfaces bulging outwards the external envelope of the shearband boudin, disposed symmetrically at opposite locations of both sides of the boudin, designated as the blunt tip (B-t) – Fig. 1. These geometries could result from mass accumulation or mechanical erosion processes directly related to the genesis of shearband boudins.

The fieldwork suggested that the asymmetry imposed by the B-t position on boudin envelope could be sensitive to the amount of deformation. In an attempt to measure this asymmetry two parameters were introduced (Fig. 1 and Table 2): d – internal displacement width (line segment defined between orthogonal projection on B_{bs} of diametric opposite B-t) and ψ – angular internal asymmetry (angular relationship that is measured as a function of the opposite B-t positions).

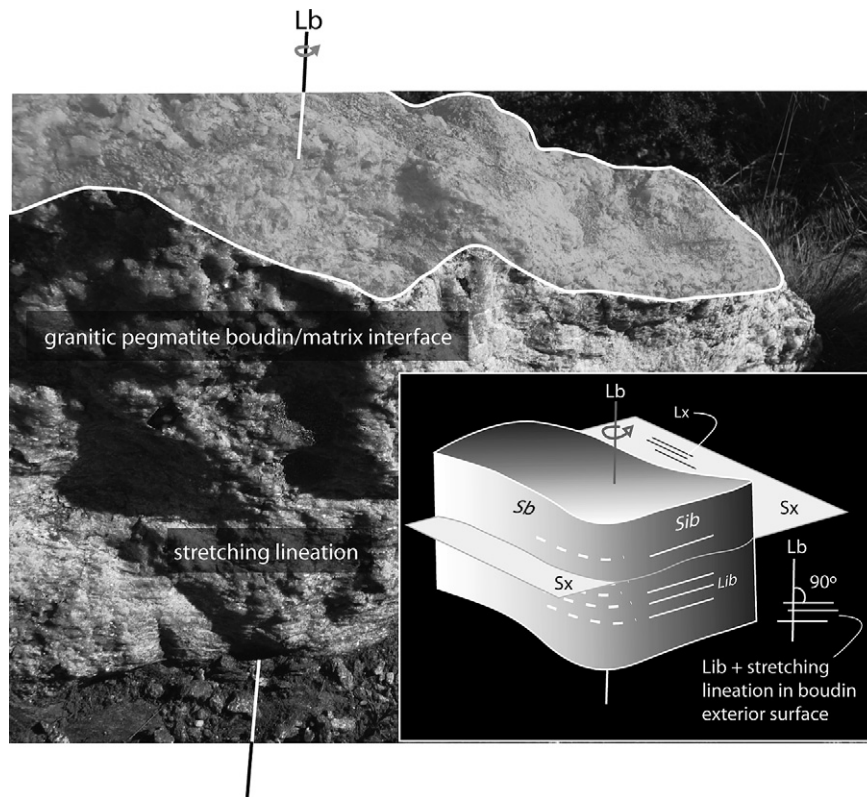


Fig. 2. Geometric relationship between the boudin axis (L_b) and the local displacement plane (S_x). It was observed that, in MLDSZ, the angle between stretching lineation (contained in S_x) and the boudin axis (L_b) is always 90° . The scheme represents the inter-boudin surface (L_{ib}) and the boudin exterior surface. Shear sense is sinistral.

The parameter Ψ' is a direct function proportional to Ψ (angular deformation), because both have limits between 0° (original layer without deformation) and 90° (maximum theoretical deformation) and respond directly to the incremental strain. However, despite being an easily measured field parameter, its behaviour during deformation is not yet well known.

2.2. Methodology

The parameters (Bbs and c' type-I) introduced in this study prove to be particularly useful for distinguishing between shearband boudins and domino boudins.

In shearband boudins, the position of the sharp tip and blunt tip is well-defined as well as the position of Bbs, which is unequivocally defined between the two opposite sharp tips (Fig. 3A). The c' type-I is always synthetic with the bulk shear sense, and a sequence of B-t, S-t, S-t, B-t tips, defined in two consecutive bodies, can be observed along a given c' type-I surface.

In the general case of domino boudins, at first sight, there are two possible orientations of the Bbs, because all the four edges of a boudin seem to be sharp tips. On domino boudins, four consecutive sharp tips are identified along the c' type-I surface, so a new notation is introduced here to identify two distinct tips: $S-t_{\text{ext}}$ for those that are in the endpoints and $S-t_{\text{int}}$ for those falling in the interior (Fig. 3B). The correct positioning of Bbs must be the one that passes through the internal opposite acute tips (Fig. 3B). A sequence of four sharp tips ($S-t_{\text{ext}}$, $S-t_{\text{int}}$, $S-t_{\text{int}}$, and $S-t_{\text{ext}}$) can be observed along a given c' surface or, in the presence of flanking structures, the same is defined but the sequence is S-t, B-t, B-t, S-t (Fig. 3C).

The field approach to the geometric analysis of shearband boudins, performed with the purpose of their description and kinematic interpretation, must be implemented using a well-defined methodology. In aiming for a universal application it is desirable to adopt a purely descriptive approach, accomplished in several steps. In the geometric analysis of shearband boudins the displacement plane (S_x) that, by definition, is perpendicular to foliation (S_n) and contains the host-rock stretching lineation (L_x), must be used, which is valid for general deformation zones with monoclinic symmetry. As L_x is not always clearly visible in the surroundings of a boudin, the observation plane to perform measures is given by L_b , using the perpendicular relationship between S_x and the boudin axis (L_b) (Fig. 2). Whenever L_b or S_x (that contains L_x) are hidden, this method cannot be applied since it is not possible to control the observation plane.

The observation of the matrix external foliation related to the development of shear zones is a *sine qua non* condition to

determine the shear zone kinematics. This foliation (S_n) is, itself, an active deformation structure and for high strain magnitudes it tends to be sub-parallel to the bulk shear plane—C plane. In general, in simple shear the foliation does not match the XY plane of the finite strain ellipsoid nor the C plane, except for high (tending to infinite) strain deformation. In the vicinity of boudins it is usual to ascribe deflection of S_n as a ductile response due to synthetic or antithetic rotation of the body. So, it is necessary to look for a measure of S_n outside the contact strain zone where S_n remains planar.

The identification of the boudin bisector surface (Bbs) is an important parameter making possible the measurement of the internal asymmetry width (d) and kinematics (Fig. 1). In simple shear, the Bbs of foliation-parallel boudin trains is rarely parallel or sub-parallel to S_n , usually showing an antithetic rotation relatively to the kinematic of the shear plane (Fig. 4A). This antithetic rotation is also valid for foliation-oblique boudin trains (Fig. 4B).

The detection of the two blunt tips (B-t) is fundamental to identifying the kinematic criteria of isolated boudins (Fig. 1). Usually, B-t corresponds to the development of a convex surface bulging into the matrix at the intersection between S_b and c' type-I. This shape could result from a mechanism of material migration due to the rotation and translation of the body. The position of B-t relatively to Bbs must define a local asymmetry, where the two blunt tips are in a diametrically opposite position, alternating with sharp tips (S-t) that are the endpoints of Bbs.

The measurement of the boudin internal asymmetry (d) requires the definition, on the Bbs line, of the intersection points with the orthogonal projection of lines connecting the maximum curvature points of the B-t surface. By definition, d is the width of the line segment defined between those intersection points (Fig. 1).

The boudin length (L) and the boudin width (W) give the dimensions of the body. The ratio L/W is often used as a characteristic feature of boudin type. The acquisition of these data must be initiated by measuring L parallel to the plane that was originally the exterior surface of the tabular body (S_b), followed by the measure of W (maximum boudin thickness), that must be orthogonal to L . In the studied shearband boudins L is generally greater than W .

The identification of c' type-I planes is made through the recognition of the links between the blunt tips (B-t) of successive shearband boudins (Fig. 3A). The effectiveness of this parameter derives from the fact that its kinematics is synthetic to the regional bulk shear plane (C plane).

The measurement of inter-boudin displacement D' (an underestimate of D useful in shearband boudins in HT simple shear zones), when observable, gives in conjunction with d , an approximation of the minimum displacement of the shear zone. It is

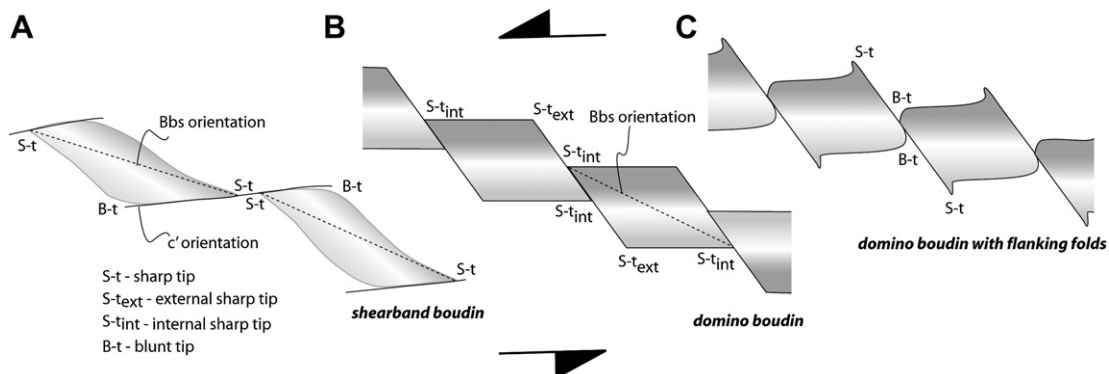


Fig. 3. Common sequences of boudin tips that were used to identify some boudin types: (A) shearband boudin (B-t, S-t, S-t, B-t); (B) domino boudin ($S-t_{\text{ext}}$, $S-t_{\text{int}}$, $S-t_{\text{int}}$, $S-t_{\text{ext}}$); (C) domino boudin with flanking folds (S-t, B-t, B-t, S-t). The shear sense is sinistral for all the types.

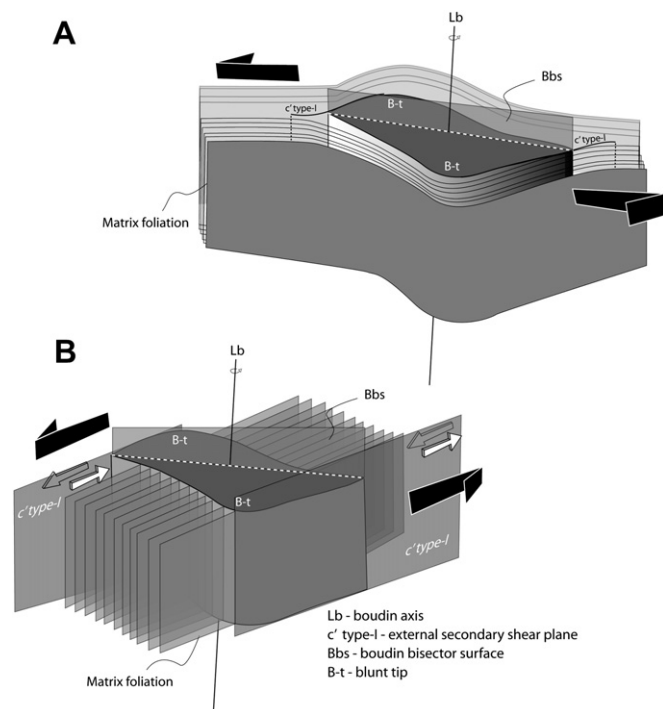


Fig. 4. Boudinage kinematic criteria – Bbs, B-t and *c'* type-I. (A) foliation-parallel boudin train; (B) foliation-oblique boudin train. Independently of original relationship between the isolated boudin and the regional foliation, Bbs, B-t and *c'* type-I orientation have similar relative position and spatial development. Shear sense is sinistral.

measured on the *c'* type-I surface, between two consecutive sharp tips (S-t) of adjacent boudins (Figs. 1 and 3A).

3. The example of Malpica-Lamego Ductile Shear Zone

3.1. Geological setting

The Malpica-Lamego Ductile Shear Zone (MLDSZ) extends ca. 275 km with an NW-SE orientation parallel to the trend of the Variscan belt of NW Iberia (Fig. 5).

This crustal tectonic structure was previously described in terms of two different strike-slip shear zone segments: The Malpica-Vigo Shear Zone in the northern part (Iglesias and Choukroune, 1980) and the Vigo-Régua Ductile Shear Zone in the southern part (Ferreira et al., 1987).

The kinematics in the northern part is well established with a multiphase movement (Llana-Funez and Marcos, 2001). Initial movement was as a complex reverse fault, 365–315 Ma (Rodríguez, 2005), coeval with the period of nappe tectonics of the second regional Variscan deformation phase (D2). Following this episode, there was a dextral strike-slip movement, 300–310 Ma (Rodríguez, 2005), related to a sub-vertical tectonic style of post-nappe tectonics during continent–continent collision, corresponding to the third regional Variscan deformation phase (D3).

In the southern part only the strike-slip movement is well recognized (e.g., Fernandes, 1961; Ferreira et al., 1987; Pereira et al., 1993; Coke et al., 2000) with a multiphase kinematic interpretation: dextral during the D1 and D2 (370–310/315 Ma) and sinistral during the D3 (310/315–300 Ma) Variscan deformation phases (Ribeiro, 1974). Holtz (1986) recognized an early thrust event (D1) followed by an episode that changed the structural vergence before the sinistral strike-slip event (D3).

The present level of exposure shows Middle Palaeozoic shear structures formed at mid-crustal levels in a strike-slip tectonic

regime. The shear zone has a regionally consistent sub-vertical and west-dipping foliation, and a sub-horizontal stretching lineation.

The western hanging wall units in contact with the MLDSZ belong to the parautochthon of the Galicia-Trás-os-Montes Zone (GTOMZ) of the Iberian Variscan Belt.

The eastern footwall rocks of the northern part of the MLDSZ belong to the allochthonous complexes of the Malpica-Tui Unit (MTU) of the GTOMZ, while in the southern part the shear zone develops along parautochthonous and autochthonous sequences of Central Iberian Zone (CIZ) and related granitic rocks, with no apparent structural gap between the border blocks.

Granodioritic porphyritic rocks, whose emplacement was structurally controlled by this crustal anisotropy, characterize all shear zone pathways, particularly at its southern tip.

In the Salgosa sector, the MLDSZ is recorded as a high temperature (HT, as defined by Scholz, 1980), heterogeneous and progressive simple shear zone, with bulk left-lateral kinematics.

The deformation zone is marked by a generalized foliation (*S_n*) defined by *Bt* + *Ms* ± *Sil* (mineral symbols according to Kretz, 1983) with a median attitude of N330°/85°W. A mineral lineation stretching marked by sillimanite fibres, plunges 10–30° to N158°.

The thermo-barometric evolution of metamorphic rocks related to the MLDSZ, after the exhumation episode of allochthonous complexes of the Malpica-Tui Unit, records a common pathway under conditions of low pressure (~0.4 GPa) and high temperature (~550 °C) compatible with the paragenetic occurrence of sillimanite instead of andalusite.

In the Salgosa sector, deformed granitic aplite-pegmatite intrusive bodies (*Qtz* + *Fk* + *Ms*, *Qtz* + *Fk* + *Ms* + *Tur*, *Qtz* + *Fk* + *Ms* ± *Tur* ± *Grt* – mineral symbols according to Kretz, 1983) and metamorphic segregation veins (*Qtz*, *Qtz* + *Ms*, *Qtz* + *And* + *Ms*, *Qtz* + *And* + *Sil* ± *Ms*) of different ages are exposed, showing structures such as shearband boudins, not always with the classical morphology or with clear kinematics.

3.2. Results and discussion

The values obtained in the study of Salgosa sector (MLDSZ) shearband boudins (number of data in database = 207), are presented in this section highlighting relative rather than absolute values, since it is hoped that they can be used for comparison purposes with other simple shear zones.

Bbs (Fig. 1) azimuths present a natural dispersion around an average value in a statistical normal distribution (Fig. 6A). Despite the relative heterogeneity of the geological environment and even some deformation partitioning, the amount of antithetic rotation of the shearband boudins (measure by the angle between Bbs and *S_n*) shows a regular trend. This fact provides statistical confidence in this parameter, which allows wider use in a kinematic approach.

The statistical analysis of dispersion of *c'* type-I orientation values shows a central tendency with a slight dispersion to the right (Fig. 6B), that allows the use of this value as a regional reference orientation, despite this asymmetry. One possible explanation for this asymmetry is the progressive parallelism with *S_n*, which possibly results from the deformation intensity.

The parameter *d* takes an absolute value, which depends on the size of the boudin, so a normalization of this value using the length *L* should be performed. The histogram of normalized *d* values (*d_{norm}*, Fig. 6C) shows a bimodal tendency, with two slightly different normalized values (0.4 and 0.6 respectively), but quite distinct absolute values. This may be the result of two different intensities of strain related to local deformation partition observed in the field, which was enhanced by ductility contrasts related to different lithological veins.

Goscombe and Passchier (2003) stated that the relationship between the boudin axial length (*L*) and width (*W*), the ratio *L/W*,

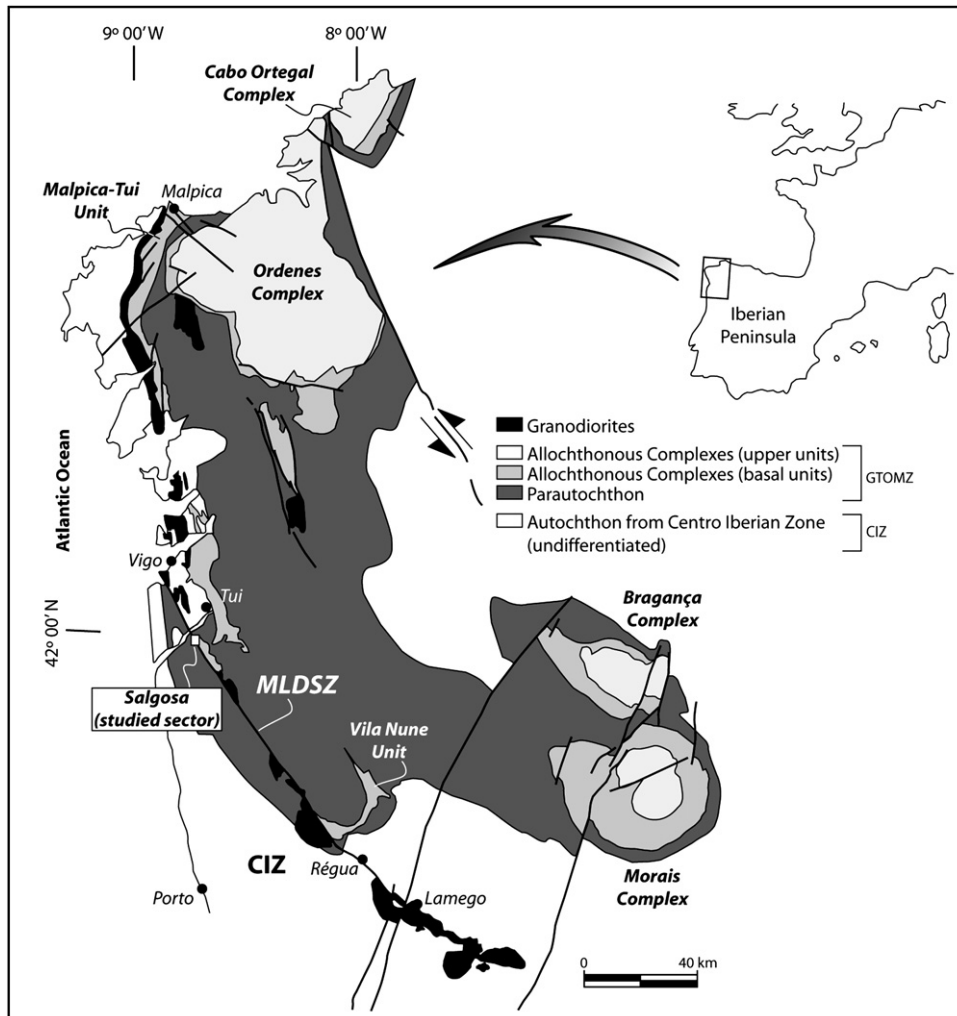


Fig. 5. Geologic sketch map of the Variscan belt of NW Iberia, with the localization of studied sector of Salgosa on the Malpica-Lamego Ductile Shear Zone (MLDSZ). This crustal structure was previously described in terms of two different strike-slip shear zone segments: Malpica-Vigo Shear Zone (Iglesias and Choukroune, 1980), in the northern part, and Vigo-Régua Ductile Shear Zone, in the southern part (Ferreira et al., 1987). CIZ – Centro Iberian Zone; GTOMZ – Galicia-Trás-os-Montes Zone. Adapted of Ribeiro et al. (1990) and Llana-Funez and Marcos (2001).

displays different average values in foliation-parallel boudin trains, in shearband boudins (average value of $L/W = 3.62$) and in domino boudins (average value of $L/W = 2.12$).

The present study shows that the axial relation L/W does not control the determination of boudin type. This finding arises from the analysis of the field data presented in Table 3. These reveal the presence of shearband boudins in a broad range of L/W , varying between 0.87 and 17.8 (average value = 3.34). This wide range of L/W ratios could be a consequence of the variable viscosity ratios between the matrix, weak metamorphic segregation veins (82% of the studied bodies), and stronger granitic aplite-pegmatite tabular bodies (18% of the studied bodies). In both cases, the rheological conditions in HT shear zones occur under high homologous temperatures (T/T_m , where T_m is the solidus temperature of the system), giving the geological materials an enhanced ability to flow and deform. A consequence of this behaviour is that W is always shorter than the width of the original layer, and L is always longer than the initial length of the boudin. It seems that the type of boudin does not depend either on its axial ratio (L/W) or on the viscosity contrast (metamorphic veins/matrix vs. aplite-pegmatites bodies/matrix), but it may depend on a not yet completely defined parameter that reflects the bulk ductility of the materials subject to deformation.

The D'/W ratio represents the displacement between boudins normalized by width. The analysis of field data in MLDSZ (Table 3) reveals the presence of shearband boudins with a broad range of D'/W , varying between 0.0 and 11.1 (mean value = 1.6). This ratio is not used in situations of overlap between adjacent shearband boudins. The values of D'/W , that correlate with the displacement along c' type-I, may have a significant influence on the evaluation of the regional extension.

The deviation from the parallelepiped geometry, defined by the acute angle between S_b and S_{ib} (θ), respectively, the long side and short side of the boudin, only gives a qualitative measure of the deformation intensity of the boudin, because there is not a straightforward relationship between this angle and the quantitative deformation parameters. In fact, in the initial stage of shearband boudin deformation, θ values are higher than in the final stages of deformation. The θ values measured in MLDSZ have a mean value of 13.8° with a standard deviation of 9.0° (Table 3).

Goscombe and Passchier (2003) use the parameters L/W and D'/W vs. θ to describe the geometry of foliation-parallel boudin trains. The relationships between these parameters (Fig. 7) can delimit the field of shearband boudins of Goscombe and Passchier (2003) and allow comparison with those studied in MLDSZ. In

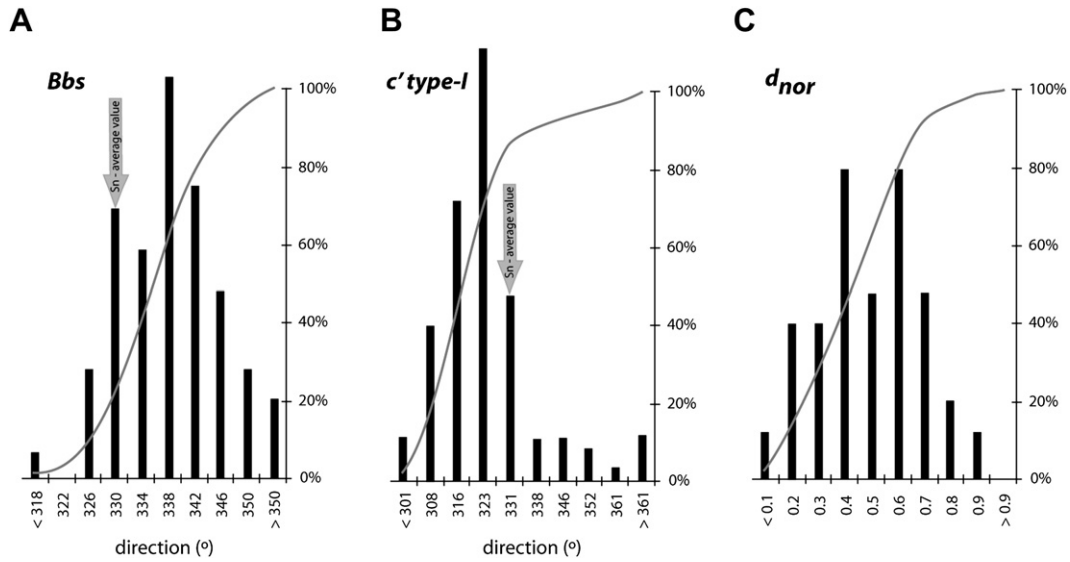


Fig. 6. Variation of the most significant geometric parameters of shearband boudins (number of data in database = 207) in MLDSZ. The histogram and the cumulative curve describe: (A) a quasi-normal distribution to Bbs; (B) a right asymmetric distribution to *c'* type-I; (C) a bimodal distribution to d_{norm} . It should be noted that 90% of data from Bbs fall in a narrow range of 20°. The orientation of *c'* type-I shows a central value well marked and a right asymmetry that could reflect its tendency to parallelise to foliation (Sn). The bimodal tendency of d_{norm} shows a high degree of overlap, which masks the possible register of the partition, for local deformation. On histograms A and B an arrow marks the average value of regional foliation (Sn) = 330°/85°W.

Fig. 7B, the data from Goscombe and Passchier (2003) were plotted using D/W values instead of D'/W , with the purpose of enabling comparison with θ values. This constraint on data projected on the vertical-axis only implies shrinkage of the points along this axis. To the above-mentioned authors the shearband boudins are characterized by values of θ between 20° and 60° and ratios of $L/W < 15$ (Fig. 7A) and $D/W < 8$ (Fig. 7B). A distinctive feature of S-slip (synthetic-slip boudinage) shearband boudins in foliation-parallel boudins trains is their low values of θ and an L/W ratio varying from low values (common to other types of boudins) to relatively high values.

Table 3

Comparison of the results obtained for shearband boudins parallel to the foliation by Goscombe et al. (2004) with those obtained in the present work. The validity of the proposed parameters is presented for the MLDSZ. Sn – foliation (main shear surface).

Parameters	Goscombe et al. (2004)	Present work (MLDSZ)
L/W	3.57 (mean)	3.34 (mean) 0.87 (min); 17.8 (max)
D/W	2.20 (mean)	1.6 (mean) 0.0 (min); 11.1 (max)
θ	39° (mean)	13.8° (mean); 9.0° (SD)
Bbs		337° (mean); 7.7° (SD)
<i>c'</i> type-I		320° (mean); 13.7° (SD)
Bbs \wedge Sn		80% (valid values)* 7.7° (mean) –14° (min); 30° (max) 84% (valid values)*; 8.3° (mean) –39° (min); 36° (max)
<i>c'</i> type-I \wedge Sn		90% (valid values)* 16.3° (mean) –37° (min); 47° (max)
Bbs \wedge <i>c'</i> type-I		98%** 98% (valid values)*; 17 cm (mean) 0.26 cm (min); 280 cm (max)
B-t		98% (valid values)*; 98% (valid values)*; 45.7° (mean); 24° (SD)
d		
ψ		

* The value is considered valid when it is coherent with kinematic interpretation.

** % of positive identification of B-t is coherent with kinematic interpretation

In the MLDSZ, Fig. 7 shows a shift of the points towards lower values of angle θ than those measured by Goscombe and Passchier (2003) and slightly higher normalized displacement, even using D'/W values. For lower θ , the ratio L/W seems to be limited by a minimum value. This generalized trend means that, probably, the deformation ratio is higher in HT shear zones (e.g., MLDSZ) than in the area studied by Goscombe et al. (2004).

Among the angular relationships that can be set between the directional parameters, the angle BbsSn (Sn is the regional matrix foliation that matches the bulk shear plane) is the most interesting from a statistical point of view, since it has a quasi-normal distribution around a central value (Fig. 8 and Table 3). Low values of this angle indicate the existence of a high degree of parallelism between the long axes of boudins and the bulk shear zone direction, a situation that, when verified, leads to some ambiguity in kinematic interpretation.

The angle *c'* type-ISn has an average value of 8.3° (Table 3) and the histogram (Fig. 6) shows a left asymmetrical distribution (negative values). These negative values are associated with boudins with ill-defined geometries that, in some cases, are the result of a complex shape evolution. The distribution of the angle Bbs \wedge *c'* type-I (Fig. 8 and Table 3) has also a left asymmetry, as a consequence of the *c'* type-I values dispersion.

4. Discussion: kinematic interpretation of boudins

The classical kinematic interpretation of asymmetric boudins requires knowledge of the sense of the slip-direction on the surface separating boudins. In order to use the asymmetric boudins as shear sense indicators (e.g., Etchecopar, 1977; Swanson, 1992; McNicoll and Brown, 1995), the identification of the bulk shear sense requires the interpretation of slip sense on this surface: synthetic-slip boudinage (S-slip) or antithetic-slip boudinage (A-slip). The approach proposed in this work is based on the observation of new parameters and relationships, overcoming this need.

The kinematic interpretation of asymmetric boudins requires measurements in the plane of the movement, i.e., in the plane perpendicular to foliation and parallel to stretching lineation.

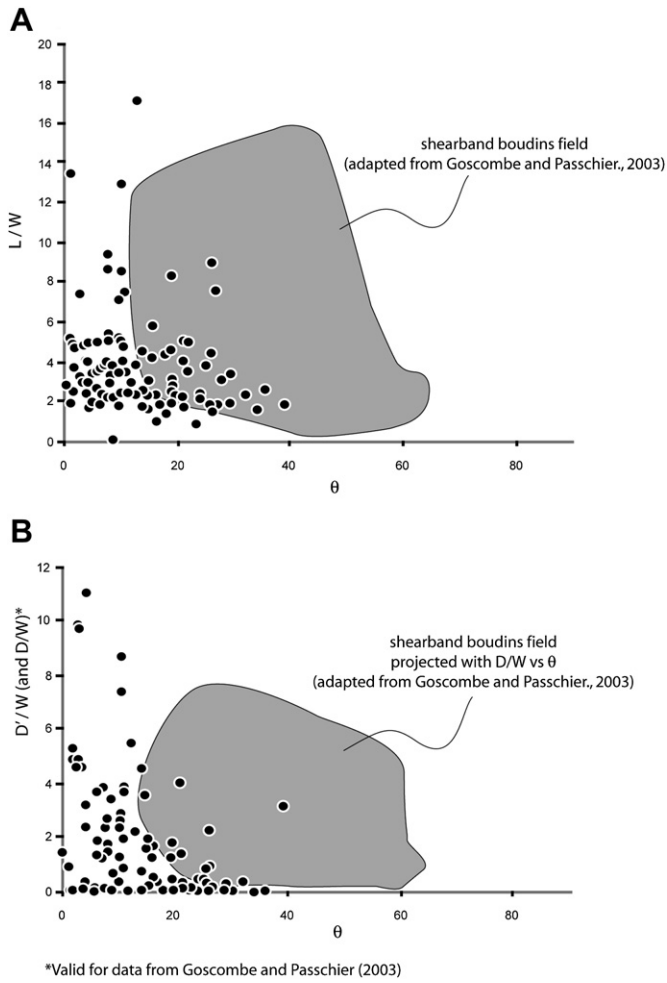


Fig. 7. Projection of the ratios from the shearband boudins in MLDSZ in comparison with the fields of shearband boudins (adapted from Goscombe and Passchier, 2003): AL/W ; $B-D'/W$ (and D/W). In order to analyse the relation of the data with θ , the ratio D/W from Goscombe et al. (2004) was projected instead of D'/W . Closed symbols indicate the data set obtained in the present study.

Among others, Goscombe and Passchier (2003) concluded that the kinematic interpretation cannot be done if the stretching lineation (Lx) is not known or if it is oblique to boudin axis (Lb). Besides, when this measurement is made in the vicinity of boudins, the mechanisms involved in boudinage could cause geometric changes in the matrix, which mask and change the regional Lx .

The coplanar relationship of Lb with a mineral stretching lineation on the boudin exterior surface and an orthogonal relationship between these two structures with Lb , indicates that Lb tends to be the π -pole of the local displacement plane Sx (Fig. 2). Consequently, this makes interpretation of the bulk kinematics possible even in the absence of a visible Sx , since Lb is relatively easy to determine in each boudin. Nevertheless, it is necessary to take precautions in the identification and measurement of Lb . These relations must be observed with care because the supporting data come from a simple shear domain with monoclinic symmetry.

In fact, the local kinematics does not necessarily correspond to the bulk kinematics, since the presence of anisotropic and heterogeneous materials results in spatial variations in the geometric and angular parameters of boudins. Therefore, shear zone kinematic analysis requires a statistical validation of each individual criterion, determined in each boudin. This procedure is beyond the scope of this paper.

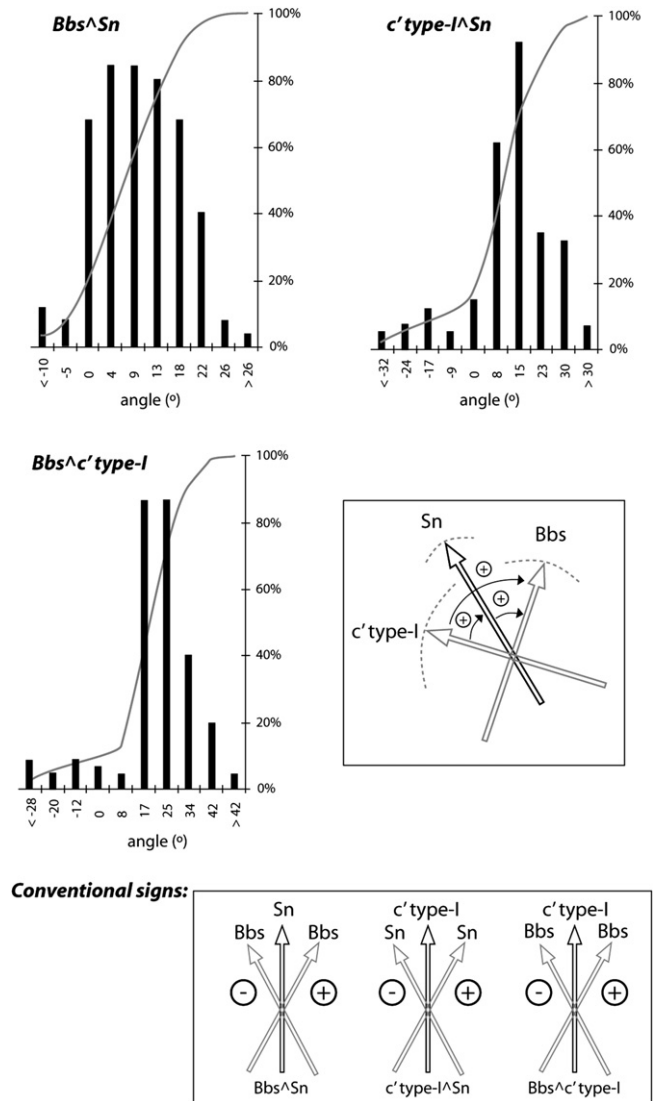


Fig. 8. Relations between typical parameters of shearband boudin for the MLDSZ sinistral shear zone. The angular relationship between Bbs, c' type-I and Sn, is generally positive; dash line represents relative standard deviation for each parameter. The conventional signs used to denote angular relationships between directional parameters are also represented.

The angle Bbs^Sn is closed to parameter θ (the angle between Sb and Sn , designed as block rotation angle) proposed by Goscombe et al. (2004). Generally, Bbs is not parallel to Sn (in the MLDSZ, Sn is coincident with the boundary of the shear zone). Thus, for foliation-parallel boudin trains, the Bbs surface suffers a rotation relative to the foliation in the host rock that is antithetic with respect to the bulk shear sense (Fig. 4A). In foliation-oblique boudin trains, the Bbs rotation is also antithetic to the kinematics of the shear zone. The angle Bbs^Sn is positive for 80% of the studied shearband boudins in the MLDSZ (Fig. 8, Table 3). Therefore, it can be concluded that clockwise rotation of shearband boudins is compatible with sinistral slip of the bulk shear zone, and vice versa. This means that clockwise rotation of the body is a successful criterion for identifying the sinistral sense of the shear zone kinematics (Fig. 8).

The internal asymmetry of shearband boudins, characterized by the existence of blunt tips (B-t), combined with the boudin bisector surface (Bbs), allows a secure criterion to identify the shear

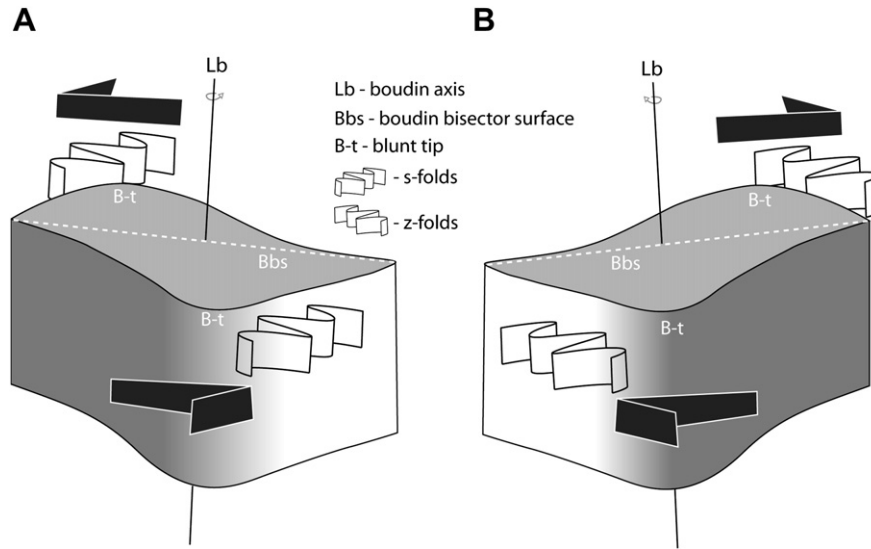


Fig. 9. Matrix crenulations (in vicinity of shearband boudins), used as kinematics criterion to boudinage. (A) left-hand boudin (s-folds) and (B) right-hand boudin (z-folds). The presence of crenulations allows confirming the interpretation of kinematic.

kinematics. Thus, after identification of the attitude of the Lb and, implicitly, Sx, the observer must look parallel to the Bbs at a sharp tip of the boudin, looking towards the interior of the boudin. If the nearest B-t is on his left-hand and the Bbs deviates clockwise from

Sn, then the shear zone has a left-hand kinematics (Fig. 4); otherwise, if the nearest B-t is on his right-hand and the Bbs deviates counter-clockwise from Sn, the shear has a right-hand kinematics. This is applicable to all the possible shear zones types, since there is

	Dextral shear zone	Sinistral shear zone
<i>Bbs orientation</i>	<p>Bbs rotated counter-clockwise relative to Sn</p>	<p>Bbs rotated clockwise relative to Sn</p>
<i>B-t relative position</i>	<p>On the right side of Bbs</p>	<p>On the left side of Bbs</p>
<i>c' type-I orientation</i>	<p>Synthetic with shear zone (rotated clockwise relative to Sn)</p>	<p>Synthetic with shear zone (rotated counter-clockwise relative to Sn)</p>
<i>Matrix crenulation (vicinity of boudin)</i>	<p>Presence of Z-folds near B-t</p>	<p>Presence of S-folds near B-t</p>

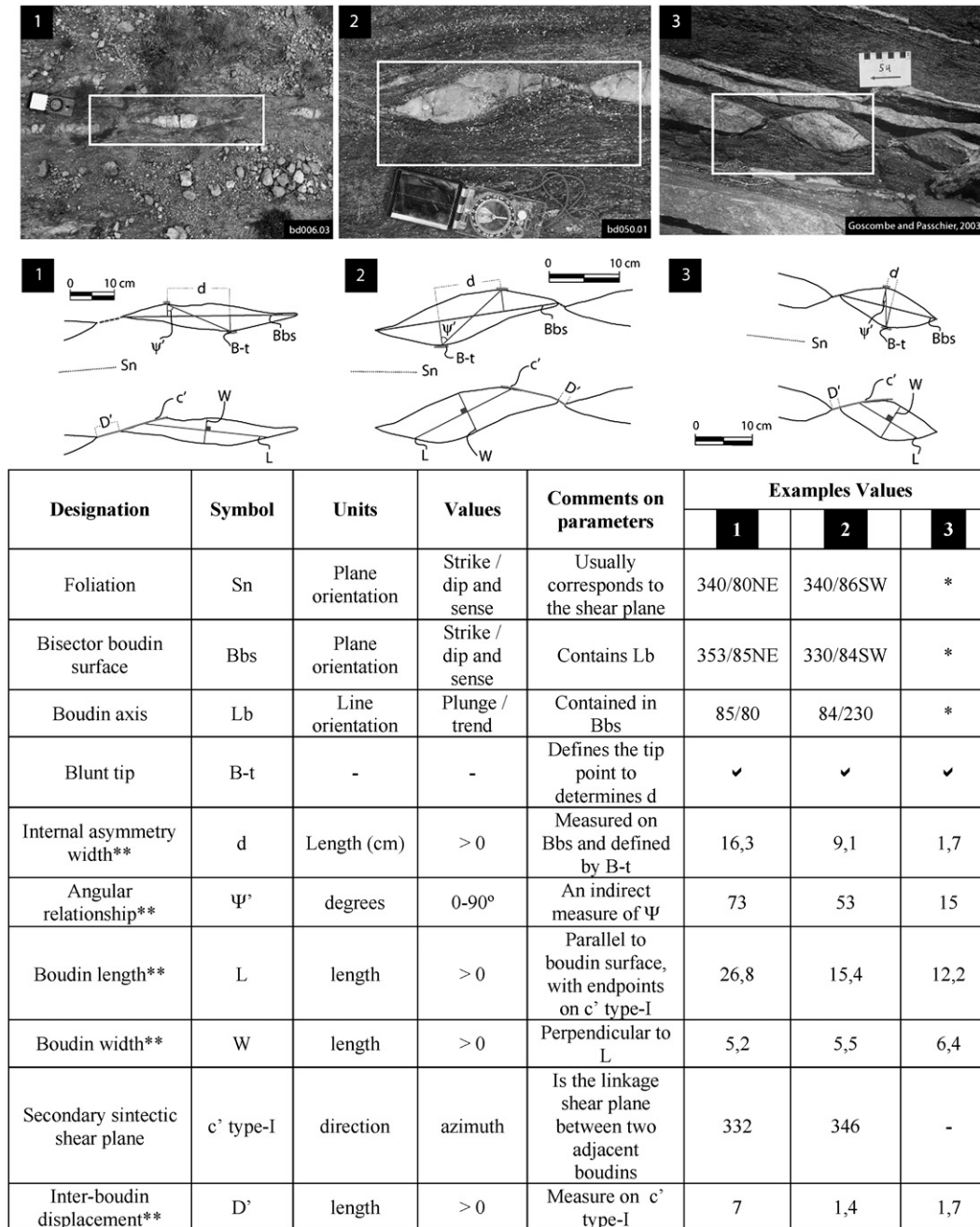
Fig. 10. Geometric criteria to determine the kinematics of the shearband boudins in strike-slip shear zones. These criteria could be used independently as a first approximation to kinematics of the boudin. However, to achieve a more consistent determination it should be, at least, checked if two of those criteria are coincident, because at HT shear zones the degree of structural breakdown could lead to a perturbation of these relationships.

coincidence between the criteria based on B-t and Bbs, i.e., the position of the B-t is well defined and agrees with the relative position of Bbs. The utilization of B-t criterion was valid to identify the true kinematics of the shear zone in 98% of the cases (Table 3).

The movement along c' type-I structure has synthetic kinematics relative to the shear zone, i.e., sinistral displacements indicate that the shear zone has left-hand kinematics. The angle c' type-I \wedge Sn in the MLDSZ, indicative of the position of c' type-I relative to the shear zone plane (since the foliation coincides with the shear

plane), is positive in 84% of the cases (Table 3), being, in most cases, coherent with the kinematics of the shear zone (Fig. 8).

The described criteria (Bbs orientation, B-t relative position and c' type-I orientation) could be used independently as a first approximation to the kinematics of the boudin. However, to achieve a more consistent determination, at least, two of these criteria should be coincident, because in HT shear zones flow complexities could lead to a perturbation of these relationships. Additionally, the determination of the shear zone displacement plane imposes



* Must be measured in the field; ** These parameters were measured parallel or sub-parallel to Lx (examples 1 and 2) and with this assumption (example 3); As an exercise to illustrate the method it was, also, assumed that photo of example 3 was taken perpendicular to the exposed boudin surface.

Fig. 11. Application examples of the proposed method to shearband boudins (sub-parallel to shear zone foliation) from different HT shear zones. 1 – MLDSZ; 2 – Porto-Tomar-Ferreira do Alentejo Shear Zone; 3 – KaoKo Belt, Namibia (Goscombe and Passchier, 2003). The kinematic analysis of all the examples using Bbs, B-t and c' type-I parameters indicates sinistral kinematic to examples 1 and 3, and dextral kinematic to example 2. In all the examples the several criteria used give the same result and are consistent with each bulk shear sense.

the identification of the statistical attitude of Lb and also of the orientation of the matrix foliation (Sn).

This approach was validated through fieldwork in the Salgosa sector of the MLDSZ, where it was successfully applied to all of the studied boudins. The results are synthesized in Table 3 and Fig. 8.

Sometimes, in the vicinity of the boudins in HT simple shear zones the matrix presents crenulations that may be useful for kinematic interpretation, as stated by Goscombe and Passchier (2003). The orientation of crenulation axes parallel to Lb can be used to identify, for example, sinistral shear movements and dextral shear movements, through the observation of s-folds and z-folds, respectively, once the outcrop orientation is taken into account (Fig. 9).

When dealing with ill-defined shearband boudins, the Bbs orientation could be the most difficult parameter to measure, especially when the angle $Bbs^{\wedge}Sn$ is low.

Fig. 10 summarizes the parameters and the kinematic criteria applied to shearband boudins in HT strike-slip shear zones.

The application of this method to different shearband boudins is illustrated in Fig. 11, with examples taken from our own fieldwork (MLDSZ and Porto-Tomar-Ferreira do Alentejo Shear Zone – Dias and Ribeiro, 1993; Fernandez et al., 2003) and from the literature (KaoKo Belt, Namibia – Goscombe and Passchier, 2003).

5. Conclusions

The proposed methodology and parameterisation of shearband boudins is useful for kinematic analysis of shearband boudins, in HT simple shear zones with monoclinic symmetry.

The new parameters have allowed trouble-free identification and measurement in boudin trains that depart from the classical original morphology, such as those studied in Salgosa sector (MLDSZ).

The key observation concerning the interpretation of boudinage is the identification of the boudin axis (Lb). Once this is resolved, the observation plane is determined by the relationship between Lb and Sx (a plane defined in this work that contains the stretching lineation in monoclinic symmetries).

The external morphology of shearband boudins in HT simple shear zones diverges from the classical parallelepipedic shape, with the development of two opposite blunt tips (B-t), truncated by secondary shear planes (c' type-I) defined between adjacent shearband boudins.

The Bbs, a directional parameter, and its angular relationships (angles $Bbs^{\wedge}Sn$ and $Bbs^{\wedge}c'$ type-I), are more suitable to measurement of shearband boudins than the direction of Sb or Sib (so, the value of angle θ) because of its irregularity and poor definition.

The utilization of d and ψ' gives a numerical quantification that could be correlated with the internal deformation (evaluated in an empirical way) in shearband boudins; the proposed ψ' parameter has a relation with the deformation similar to the angular deformation parameter ψ .

The measurement of inter-boudin displacement, D' (component of boudin external deformation), an underestimate of D , gives in conjunction with d (the component of boudin internal deformation) an approximation to the minimum regional displacement.

In shearband boudins in HT simple shear zones, the values of L and W represent the width and the length of the boudin body, but rarely are the width and length of original bodies, as in domino boudins where these parameters could be defined without doubt. Although the ratio L/W and the θ parameter can give, a quantification of the internal deformation of boudin bodies, in HT simple shear zones they are not sufficient because they aren't sensitive to the most important features of boudin internal deformation: the bulging and asymmetric position of the blunt tips, that we propose to measure with an angle (ψ') and a length (d).

The kinematic interpretation of shearband boudins using the proposed parameters is made taking into account the Bbs orientation (which rotates antithetically relative to the bulk shear sense), c' type-I kinematics (synthetic to the bulk shear sense) and the relative position of B-t and Bbs (on the right side this means dextral bulk shear, and vice versa).

Acknowledgements

Partial funding to JP was provided by the Centro de Investigação Geológica, Ordenamento e Valorização de Recursos that is supported by the Pluriannual program of the Fundação para a Ciência e a Tecnologia, funded by the European Union (FEDER program) and the national budget of the Portuguese Republic. Very insightful and helpful reviews were done by C. Fernández (University of Huelva) and two reviewers, for which we are grateful. We want to acknowledge to T. Valente (University of Minho) for her suggestions that helped to simplify the manuscript structure and to A. McCaig (University of Leeds) for his final comments and English revision that significantly improved this manuscript.

References

- Arslan, A., Passchier, C.W., Koehn, D., 2008. Foliation boudinage. *Journal of Structural Geology* 30, 291–309.
- Bons, P., Druguet, E., Hamann, I., Carreras, J., Passchier, C.W., 2004. Apparent boudinage in dykes. *Journal of Structural Geology* 26, 625–636.
- Bosworth, W., 1984. The relative roles of boudinage and “structural slicing” in the disruption of layered rock sequences. *Journal of Geology* 92, 447–456.
- Cloos, E., 1947. Boudinage. *Transactions of the American Geophysical Union* 28 (4), 626–632.
- Coke, C., Dias, R., Ribeiro, A., 2000. Malpica-Lamego shear zone: a major crustal discontinuity in the Iberian Variscan fold belt. In: *Variscan-Appalachian Dynamics: The Building of the Upper Paleozoic Basement. Basement Tectonics*, vol. 15. A Coruña, Program and Abstracts, pp. 208–210.
- Dias, R., Ribeiro, A., 1993. Porto-Tomar Shear Zone, a major structure since the beginning of the Variscan orogeny. *Comunicações dos Serviços Geológicos de Portugal* 79, 31–40.
- Eshelby, J.D., 1957. The determination of the elastic field of an ellipsoidal inclusion and related problems. *Proceedings of the Royal Society of London A241*, 376–396.
- Etchecopar, A., 1977. A plane kinematic model of progressive deformation in a polycrystalline aggregate. *Tectonophysics* 39, 121–139.
- Fernandes, A.P., 1961. O vale de fractura de Rio Forno-Padronelo-Amarante. *Boletim do Museu e Laboratório Mineralógico e Geológico da Universidade de Lisboa* 9, 138–147.
- Fernandez, F.J., Chaminé, H.J., Fonseca, P.E., Munhá, J.M., Ribeiro, A., Aller, J., Fuentefuentes, M., Borges, F.S., 2003. HT-fabrics in a garnet-bearing quartzite from Western Portugal: geodynamic implications for the Iberian Variscan Belt. *Terra Nova* 15, 96–103.
- Ferreira, N., Iglesias, M., Noronha, F., Pereira, E., Ribeiro, A., Ribeiro, M.L., 1987. Granitoides da zona Centro-Ibérica e seu enquadramento geodinâmico. In: *Bea, F., Carnicero, A., Gonzalo, J.C., Lopes Plaza, M., Rodriguez Alonso, M.D. (Eds.), Geología de los granitoides y rocas asociadas del Macizo Hespérico (Libro de homenaje a García Figueirola)*. Editorial Rueda, Madrid, pp. 37–51.
- Ghosh, S., Ramberg, H., 1976. Reorientation of inclusions by combination of pure and simple shear. *Tectonophysics* 34, 1–70.
- Ghosh, S.K., Sengupta, S., 1999. Boudinage and composite boudinage in superposed deformation and syntectonic migmatization. *Journal of Structural Geology* 21, 97–110.
- Goscombe, B.D., Passchier, C.W., 2003. Asymmetric boudins as shear sense indicators – an assessment from field data. *Journal of Structural Geology* 25, 575–589.
- Goscombe, B.D., Passchier, C.W., Hand, M., 2004. Boudinage classification: end-member boudin types and modified boudin structures. *Journal of Structural Geology* 26, 739–763.
- Holtz, F., 1986. Chevauchement et décrochement superposés dans le socle centro-ibérique: le lineament de Ponte de Lima (NW du Portugal). *CR Académie des Sciences, Paris* 303 (sér II), 1041–1046.
- Iglesias, M., Choukroune, P., 1980. Shear zones in the Iberian Arc. *Journal of Structural Geology* 2, 63–68.
- Jeffery, G.B., 1922. The motion of ellipsoidal particles immersed in a viscous fluid. *Proceedings of the Royal Society of London A* 120, 161–179.
- Kretz, R., 1983. Symbols for rock forming minerals. *American Mineralogist* 68, 277–279.
- Llana-Funez, S., Marcos, A., 2001. The Malpica-Lamego line: a major crustal-scale shear zone in the Variscan Belt of Iberia. *Journal of Structural Geology* 23, 1015–1030.
- Lohest, M., Stainier, X., Fourmarier, P., 1908. Compte rendu de la session extraordinaire de la Société Géologique de Belgique, tenue à Eupen et à Bastogne les

- 29, 30 et 31 Août e le 1, 2 et 3 Septembre 1908. *Annale de la Société Geologique de Belgique* 35, B351–B434.
- Mandal, N., Chakraborty, C., Samanta, S.K., 2000. Boudinage in multilayered rocks under layer-normal compression: theoretical analysis. *Journal of Structural Geology* 22, 373–382.
- McNicoll, V.J., Brown, R.L., 1995. The Monashee décollement at Cariboo Alp, Southern flank of the Monashee complex, southern British Columbia, Canada. *Journal of Structural Geology* 17, 17–30.
- Paterson, M.S., Weiss, L.E., 1961. Symmetry concepts in the structural analysis of deformed rocks. *Geological Society of America Bulletin* 72, 841–882.
- Pereira, E., Ribeiro, A., Meireles, C., 1993. Cisalhamentos hercínicos e controlo das mineralizações de Sn-W, Au e U na Zona Centro Ibérica, em Portugal. *Cadernos Laboratório Xeológico de Laxe, Coruna* 18, 89–119.
- Price, N.J., Cosgrove, J.W., 1990. *Analysis of Geological Structures*. Cambridge University Press, 502 pp.
- Rambousek, C., Grasemann, B., Petrakakis, K., Iglseder, C., Zamonlyi, A., 2005. Automated image analysis of microstructures from the detachment mylonites of the Serifos Metamorphic Core Complex (Greece). *Geophysical Research Abstracts* 7, 05325.
- Reddy, S.M., Buchan, C., 2005. Constraining kinematic rotation axes in high-strain zones: a potential microstructural method? In: Gapais, G., Brun, J.P., Cobbold, P.R. (Eds.), *Deformation Mechanism, Rheology and Tectonics: From Minerals to the Lithosphere*. Geol. Soc. London, Spec. Public., vol. 243, pp. 1–10.
- Ribeiro, A., Pereira, E., Dias, R., 1990. Central Iberian zone: allochthonous sequence. In: Dallmeyer, R.D., Martinez Garcia, E. (Eds.), *Pre-mesozoic Geology of Iberia*. Springer-Verlag, Berlin, pp. 220–236.
- Ribeiro, A., 1974. Contribution à l'Étude de Trás-os-Montes oriental. *Memória dos Serviços Geológicos de Portugal* 24, 168.
- Rodrigues, B.C., Fernandez, C., Borges, F.S., 1999. Petrofabric analysis of polymineralic mylonites – The shear zone granite, Ponte de Lima, NW Portugal. In: *International Conference of Textures and Physical Properties of Rocks*. Göttingen, 199 (Abstract Volume). *Göttinger Arbeit Geol. Paleontol.*, vol. Sb4, pp. 24–26.
- Rodriguez, J., 2005. Recristalización y Deformación de Litologías Supracorticales Sometidas a Metamorfismo de Alta Presión (Complejo de Malpica-Tuy, NO del Macizo Ibérico). *Serie Nova Terra, Laboratorio Xeológico de Laxe* 29, 572.
- Scholz, C.H., 1980. Shear heating and the state of stress on faults. *Journal of Geophysical Research* 85 (B11), 6174–6184.
- Sintubin, M., Urai, J., 2007. About boudins, veins and moullions. Ther Ardenne-Eifel region (Belgium, Germany): a natural laboratory to study brittle-ductile deformation behaviour in the middle crust (abstract). In: *The Peach and Horne Meeting*, Ullapool.
- Swanson, M.T., 1992. Late Acadian-Alleghenian transpressional deformation: evidence from asymmetric boudinage in the Casco Bay area, coastal Maine. *Journal of Structural Geology* 14, 323–341.
- Treagus, S.H., Lan, L., 2004. Deformation of square objects and boudins. *Journal of Structural Geology* 26, 1361–1376.
- Wegman, C.E., 1932. Note sur le boudinage. *Bulletin de la Société Geologique de France* 52, 477–491.